Biogeosciences Discuss., 12, 20179–20222, 2015
www.biogeosciences-discuss.net/12/20179/2015/
doi:10.5194/bgd-12-20179-2015

Biogeosciences Discussions
Open Access
EGU

Succession within the prokaryotic communities during the VAHINE mesocosms experiment in the New Caledonia lagoon

U. Pfreundt[1], F. Van Wambeke[2], S. Bonnet[2,3], and W. R. Hess[1]

[1]University of Freiburg, Faculty of Biology, Schaenzlestr. 1, 79104 Freiburg, Germany
[2]Aix Marseille Université, CNRS/INSU, Université de Toulon, IRD, Mediterranean Institute of Oceanography (MIO) UM110, 13288, Marseille, France
[3]Institut de Recherche pour le Développement, AMU/CNRS/INSU, Université de Toulon, Mediterranean Institute of Oceanography (MIO) UM110, 13288, Marseille-Noumea, France-New Caledonia

Received: 4 December 2015 – Accepted: 6 December 2015 – Published: 18 December 2015

Correspondence to: W. R. Hess (wolfgang.hess@biologie.uni-freiburg.de)

Published by Copernicus Publications on behalf of the European Geosciences Union.

Abstract

N_2 fixation fuels ~ 50 % of new primary production in the oligotrophic South Pacific Ocean. The VAHINE experiment has been designed to track the fate of diazotroph derived nitrogen (DDN) and carbon within a coastal lagoon ecosystem in a comprehensive way. For this, large-volume (~ 50 m^3) mesocosms were deployed in the New Caledonia lagoon and were intentionally fertilized with dissolved inorganic phosphorus (DIP) to stimulate N_2 fixation. This study examined the temporal dynamics of the prokaryotic community together with the evolution of biogeochemical parameters for 23 consecutive days in one of these mesocosms (M1) and in the Nouméa lagoon using MiSeq 16S rRNA gene sequencing. We observed clear successions within M1, some of which were not mirrored in the lagoon. The dominating classes in M1 were alpha- and gammaproteobacteria, cyanobacteria (mainly *Synechococcus*), eukaryotic microalgae, on days 10 and 14 Marine Group II euryarchaea, on days 12–23 also *Flavobacteriia*. Enclosure led to significant changes in the M1 microbial community, probably initiated by the early decay of *Synechococcus* and diatoms. However, we did not detect a pronounced bottle effect with a copiotroph-dominated community. The fertilization with ~ 0.8 µM DIP on day 4 did not have directly observable effects on the overall community within M1, as the data samples obtained from before and four days after fertilization clustered together, but likely influenced the development of individual populations later on, like *Defluviicoccus*-related bacteria and UCYN-C type diazotrophic cyanobacteria. Growth of UCYN-C led to among the highest N_2 fixation rates ever measured in this region and enhanced growth of nearly all abundant heterotrophic groups in M1. We further show that different *Rhodobacteraceae* were the most efficient heterotrophs in the investigated system and we observed niche partitioning within the SAR86 clade. Whereas the location in- or outside the mesocosm had a significant effect on community composition, the temporal effect was significantly stronger and similar in both locations, suggesting that overarching abiotic factors were more influential than the enclosure. While temporal community changes were evident, prokaryotic diversity

BGD
12, 20179–20222, 2015

(Shannon Index) only declined slightly from ~ 6.5 to 5.7 or 6.05 in the lagoon and M1, respectively, throughout the experiment, highlighting the importance of multiple and varying sources of organic matter maintaining competition.

1 Introduction

The South West Pacific ocean is recognized as an area with one of the highest dinitrogen (N_2) fixation rates in the global ocean (Garcia et al., 2007; Luo et al., 2012). In this region, plankton taxa capable of N_2 fixation (N_2-fixing or diazotrophic organisms) are very diverse (Moisander et al., 2010) and fuel up to 60 % of the primary production (Bonnet et al., 2015a), yet their interactions with surrounding planktonic communities are rarely studied. Within this vast oceanic region, most of the studies regarding the coupling between phytoplankton and heterotrophic bacteria have targeted the Nouméa lagoon, New Caledonia. Phytoplankton and bacterial production shows seasonal patterns, with maxima in December and January and an annual heterotrophic bacterial production representing 21 to 34 % of primary production (Torréton et al., 2010). High N_2 fixation rates are a recurrent feature in the Nouméa lagoon (Biegala and Raimbault, 2008; Garcia et al., 2007), and diazotroph-derived N (DDN) was shown to be significantly channeled through the heterotrophic bacterial compartment in this environment (Berthelot et al., 2015; Bonnet et al., 2015a). Yet, no information is available on the potential effects of this N_2 fixation on bacterial successions.

The production and quality of varying sources of organic matter is expected to vary as blooms of diazotrophic organisms are transient events. Such variation is expected to influence not only biogeochemical fluxes, but also the succession of different heterotrophic bacteria, according to their metabolic capabilities. Indeed, the importance of quality and quantity of dissolved organic matter (DOM) in structuring bacterioplankton communities has been well established (Alonso-Sáez and Gasol, 2007; Beier and de Albuquerque, 2015), either by comparing the continuum of trophic conditions in situ (West et al., 2008), or following phytoplankton blooms under natural (Teeling

BGD
12, 20179–20222, 2015

et al., 2012) or experimental (Lebaron et al., 2001) conditions. Since the 1970s, heterotrophic bacterial succession during phytoplankton blooms has been observed with culture-dependent techniques (Fukami et al., 1981a) and linked to the possible origin of DOM sources (release, lysis, sloppy feeding, degradation of phytoplankton detritus), DOM size (low or high-molecular weight molecules), or quality (Biddanda and Pomeroy, 1988; Murray et al., 2007; Nagata, 2000; Riemann et al., 2000).

The VAHINE experiment (Bonnet et al., 2015b) provided a unique opportunity to study the fate of DDN in the marine planktonic food web and the interactions between phytoplankton and heterotrophic bacteria by simultaneously addressing biogeochemical parameters, stocks and fluxes, as well as biodiversity based on 16S rRNA gene sequencing and flow cytometry cell counts.

After fertilization with dissolved inorganic phosphorus (DIP), $\sim 0.8\,\mu mol\,L^{-1}$ on the evening of day 4, to alleviate any potential limitation often observed in the region (Moutin et al., 2007), two periods of about 10 days each (P1 and P2, see description in Sect. 2.1) were clearly identified in terms of diazotroph succession. During the first period, diatom–diazotroph associations (DDAs) were dominating (Turk-Kubo et al., 2015) the diazotrophic community with N_2 fixation rates decreasing from 17.9 ± 2.5 to $10.1 \pm 1.3\,nmol\,N\,L^{-1}\,d^{-1}$ (Bonnet et al., 2015a). Unicellular N_2-fixing cyanobacteria of the UCYN-C type (*Cyanothece*-like) dominated the diazotroph community in the mesocosms during the second period, but did not appear in Nouméa lagoon waters (Turk-Kubo et al., 2015). N_2-fixation rates increased during days 15–23 and reached $> 60\,nmol\,N\,L^{-1}\,d^{-1}$, which are among the highest rates measured in marine waters (Bonnet et al., 2015a; Luo et al., 2012). These two periods corresponded to characteristic successions in phytoplankton taxa, chlorophyll stocks, primary and heterotrophic bacterial production, discussed in detail in companion studies in this issue (Berthelot et al., 2015; Leblanc et al., 2015; Van Wambeke et al., 2015).

In this manuscript we focus on prokaryotic community dynamics and possible parallels between or successions among different groups of phytoplankton, heterotrophic bacteria and N_2-fixing organisms.

BGD
12, 20179–20222, 2015

2 Material and methods

2.1 Mesocosm description, sampling strategy and stocks/fluxes analyses

Three large mesocosms (~ 50 m^3) were deployed in the nutrient-poor waters of the Nouméa lagoon close to the Boulari passage (22°29.073 S – 166°26.205 E), 28 km off the coast from 13 January to 4 February 2013. Details of the location, deployment and sampling strategy are described in (Bonnet et al., 2015b). The three triplicate mesocosms were fertilized with ~ 0.8 µM KH_2PO_4 between day 4 and day 5 of the experiment to promote a diazotroph bloom. Samples were collected every morning at 07:00 a.m. over a period of 23 days from 3 selected depths (1, 6, 12 m) in each mesocosm (M1, M2 and M3) and in surrounding waters (hereafter referred to as Nouméa lagoon waters). Further details regarding the sampling are given separately (Pfreundt et al., 2015; Van Wambeke et al., 2015).

Subsampling and analysis procedures for stocks and fluxes are not given in detail here as they were mainly used for statistical analyses (see Sect. 2.3) but they are described in full in companion papers from this issue: Inorganic nutrients and chlorophyll *a* (chl) concentrations, DIP turnover time, N_2 fixation rates and primary production (PP) were analyzed according to procedures detailed in (Berthelot et al., 2015). *Synechococcus* and *Prochlorococcus* cell numbers were counted by flow cytometry (Leblanc et al., 2015). Heterotrophic bacterioplankton abundances were also determined by flow cytometry and corresponded to the sum of cells with high and low nucleic acid content, discarding autotrophic cell counts (Van Wambeke et al., 2015). Heterotrophic bacterial production (BP) was determined by the ^{3}H leucine technique, and alkaline phosphatase activity (APA) was determined on the total fraction (i.e., unfiltered samples) using MUF-P substrate (Van Wambeke et al., 2015). Three periods of the experiment were defined. P0 was defined as days 2–4, before DIP fertilization of the mesocosms. P1 (days 5–14) was characterized by DIP availability and correspondingly lower APA inside the mesocosms (Van Wambeke et al., 2015). P2 (days 15–23) was characterized by increasing chl *a* concentrations, N_2 fixation rates, PP and BP inside

BGD
12, 20179–20222, 2015

the mesocosms and also in the Nouméa lagoon, albeit to a lower extent. Further, APA increased steeply corresponding to DIP becoming limiting in the mesocosms during P2 (Berthelot et al., 2015; Van Wambeke et al., 2015).

2.2 16S rRNA gene amplicon sequencing and OTU clustering

DNA was extracted from seawater samples collected as described in Sect. 2.1 every two days at 1 and 12 m depth in M1 and in Nouméa lagoon waters. A volume of 10 L was pre-filtered through a 1 mm mesh to keep out large eukaryotes and filtered on 0.45 µm pore size, 47 mm diameter polyethersulfone filters (Pall Supor), immersed in RNA resuspension buffer (10 mM NaAc pH 5.2, 200 mM D(+)-sucrose, 100 mM NaCl, 5 mM EDTA) and snap frozen in liquid N_2. Tubes with filters were vortexed, then agitated in a Precellys bead beater (Peqlab, Erlangen, Germany) 2 × (2 × 15 s) at 6500 rpm after adding 0.25 mL glass beads (0.10–0.25 mm, Retsch, Frimley, UK) and 1 mL PGTX (39.6 g phenol, 6.9 mL glycerol, 0.1 g 8-hydroxyquinoline, 0.58 g EDTA, 0.8 g NaAc, 9.5 g guanidine thiocyanate, 4.6 g guanidine hydrochloride, H_2O to 100 mL; Pinto et al., 2009). RNA and DNA was extracted simultaneously by adding 0.7 mL chloroform, vigorous shaking, incubation at 24 °C for 10 min and subsequent phase separation by centrifugation. RNA and DNA was retained in the aqueous phase, precipitated together and stored at −80 °C for further use for metatranscriptomics analysis (Pfreundt et al., 2015) and 16S tag sequencing. For the latter, ∼ 100 ng of RNase treated total DNA was sent to a commercial provider (LGC Genomics, Berlin, Germany) for amplicon sequencing with primer pair S-D-Bact-0341-b-S-17/S-D-Bact-0785-a-A-21 (Klindworth et al., 2013), that targets bacteria and archaea. Briefly, 16S hypervariable regions 3–4 were amplified and the amplicons sequenced on a MiSeq (Illumina) sequencer, generating between 31 466 and 749 629 paired-end reads (2 × 300) per sample.

All bioinformatics steps were done using the USEARCH package and following the UPARSE pipeline (Edgar, 2013) unless mentioned otherwise. Briefly, lowest quality tails were truncated from all reads and the paired reads merged using the -fastq_mergepairs command and yielding between 25 221 and 604 457 reads of average length > 400 nt

BGD
12, 20179–20222, 2015

per sample. Merged reads were then quality filtered, reads shorter than 350 nt discarded, and converted to fasta. All fasta files were concatenated for OTU clustering, with the following steps: dereplication at 100 % identity and keeping information on the weight of each unique sequence, sorting of unique sequences by decreasing weight and discarding of singletons (weight = 1), clustering into OTUs with the -cluster_otus command using a maximum dissimilarity of 2 %. The last step includes chimera filtering (Edgar, 2013). Finally, the merged reads from the different samples were mapped back onto the generated OTUs using vsearch v1.1.3 (Rognes et al., 2015) with at least 98 % identity to create the final OTU table. For taxonomic classification of the OTUs, they were submitted to https://www.arb-silva.de/ngs/ and classified using the SILVA SSU taxonomy and database release SSU 119.1 (Quast et al., 2013). Cyanobacterial OTUs that SILVA had only classified to family level were manually curated by BLASTN searches of these OTUs against NCBI nt. If a hit with > 95 % sequence identity was found, the genus of this classification was added to the OTU table. For all further use, relative OTU abundances in each sample were calculated.

To calculate pseudo-absolute cell numbers from these relative OTU abundances, for each sample the cumulated relative abundances of *Synechococcus* and *Prochlorococcus* were divided by the respective sum of *Synechococcus* and *Prochlorococcus* cytometric cell counts, producing a sample-specific ratio (%16S/cell). We used these two groups, because flow cytometry is well-established for them and we could expect them to be reasonably precise. This ratio was then used to calculate cell numbers for all investigated phylogenetic groups by dividing their relative abundance in each sample by the sample-specific ratio.

The Shannon index as a measure of diversity was calculated separately for M1 and Nouméa lagoon waters using the *diversity* function in the R package vegan (Oksanen et al., 2015).

BGD
12, 20179–20222, 2015

2.3 Multivariate statistics of 16S community data, samples and environmental data

A canonical correspondence analysis (CCA) (XLSTATS Excel software) was used to test for significant effects of biogeochemical parameters on variations in the 16S-community structure. These parameters were PP, BP, Chl, APA, DIP, N_2 fixation rates, particulate organic carbon concentrations (POC) and temperature (T). CCA generates ordination axes which are linear combinations of the environmental variables that best explain microbial diversity composition data (ter Braak, 1986). The variables were the log-transformed biogeochemical stocks and fluxes, the objects were the 34 dominating OTUs in terms of abundance (expressed in relative OTU abundance), and the sites were sampling time and origin of the samples.

Non Metric Multidimensional Scaling (NMDS) was used to find the best display of differences in 16S community structures. The full OTU table containing relative abundances of each OTU per sample, with samples as rows and species as columns, was used for unconstrained ordination with the R package vegan (Oksanen et al., 2015). Additionally, the same procedure was run with the subset tables containing only "heterotroph" OTUs (i.e. all that were not classified as *Cyanobacteria* or chloroplasts) or only "autotroph" OTUs (i.e. all classified as chloroplasts or *Cyanobacteria* without *Melainabacteria*). First, the abundances were standardized using Wisconsin double standardization, which divides abundances by the species maximum and then standardizes samples to equal totals. This converts abundances per species into relative values and therefore reduces the weight of dominant species and increases the weight of rare species. Then, Bray–Curtis distance matrices were computed and an NMDS ordination calculated using metaMDS. MetaMDS did not use any further transformations or standardizations. Assuming that samples of day 2–8, day 10–16, and day 18–21 cluster together, ellipses were drawn using the standard error for each cluster in the ordination plot with a confidence limit of 0.95. Like this, we could consider clusters with non-overlapping ellipses as significantly different from each other at a significance level

BGD
12, 20179–20222, 2015

alpha = 0.05. Permutational Multivariate Analysis of Variance (PERMANOVA) was conducted using the adonis function in the R package vegan on the Bray–Curtis distance matrices described above. We tested the dependence of sample distances on the factors *location* (M1 or lagoon waters), *depth* (1 or 12 m) and *time* (separation of samples into three phases: day 2–8, 10–16, 18–21).

3 Results

3.1 Biogeochemical context

Here, we present data on the prokaryotic community in M1 and the Nouméa lagoon from depths of 1 and 12 m, which was close to the bottom of the mesocosm. As a foundation for understanding and discussing these data, selected biogeochemical parameters are shown in Figs. 1 and 2c and d for the corresponding sampling locations. On the evening of day 4, M1 was fertilized with ~ 0.8 µM DIP, leading to lower APA than in the lagoon until day 19, when APA in M1 increased steeply (Figs. 1c and 2c) and DIP turnover times dropped below initial levels (Van Wambeke et al., 2015). Of the three mesocosms, M1 was the one with the lowest increase of chl *a* during P2, still reaching higher levels than in Nouméa lagoon waters, whereas PP in M1 did not exceed the values measured in the lagoon (Fig. 1a and b). BP exhibited two prominent peaks in M1 with a 4-fold and 2-fold increase, on day 4 and on day 21, and was otherwise close to values measured for Nouméa lagoon waters, only slightly exceeding them on most days after day 11 (Fig. 1d).

3.2 Bacterial community based on 16S tag MiSeq sequencing

3.2.1 An overview

We identified a total of 3600 OTUs belonging to bacteria, archaea, and chloroplasts using 16S rRNA gene sequencing data from all samples combined (17 samples from

BGD
12, 20179–20222, 2015

M1, 20 samples from the Nouméa lagoon, Supplement). In the following, the term "16S community" will be used for the entirety of all 16S reads belonging to these OTUs. On this basis, the Shannon index as a measure for overall diversity was calculated. With values between 5.6 and 7 at both investigated depths over the 23 days experiment, it was relatively high. Values above 5 have been reported for the edge of the South Pacific gyre (Yin et al., 2013), but based on clone libraries, which might underestimate diversity. Over the course of the experiment we observed a slight decrease in diversity both in M1 and in the lagoon (Fig. S1 in the Supplement).

The dominating classes in M1 were alpha- and gammaproteobacteria, cyanobacteria, chloroplasts, Marine Group II (MGII) euryarchaea (*Thermoplasmata*, mainly days 10 and 14), and on days 12–23 also *Flavobacteriia* (Fig. 3a). Of these, alpha- and gammaproteobacteria exhibited clearly different dynamics between M1 and the lagoon with completely different peaking times, whereas cyanobacteria, chloroplasts and MGII euryarchaea showed similar trends (Figs. 3a and 4a, correlations in Fig. S2a in the Supplement).

Amongst the classes contributing less than 5 % to the total 16S community, dynamics were generally different between M1 and the lagoon (Fig. S2b). Inside M1, *Deferribacteres* and *Deltaproteobacteria* abundance decreased from $> 1.2\,\%$ to $< 0.7\,\%$ of the 16S community after the DIP fertilization and increased again when DIP concentrations fell below 0.1 nM on day 12 (Fig. 3c). *Cytophagia* and *Flavobacteriia* also increased at the same time, while *Actinobacteria* and *Phycisphaerae* increased on day 20 (Fig. 3b). Except for the increase in *Flavobacteriia* and cyanobacteria (predominantly *Synechococcus*), none of these late-phase increases were observed in the lagoon, although several of the less abundant classes (*Cytophagia*, *Betaproteobacteria*, *Actinobacteria*) more than doubled from day 16 to 18 in the lagoon, but also decreased just as quickly after that (Fig. 4b).

BGD
12, 20179–20222, 2015

3.2.2 Heterotrophic bacteria

As alpha- and gammaproteobacterial 16S abundances showed close to zero correlation between M1 and the lagoon (Fig. S2a), we examined the dynamics within these classes at family level. We observed clear successions within M1 that were not mirrored in the lagoon (Figs. 3c and d, 4c and d). Already on day 4 (two days after the mesocosms had been closed around the water column), the relative share of *Rhodobacteraceae* 16S tags increased from 3.5 to 12.5 % in M1, exhibiting the most extreme dynamics of all families (Fig. 3c). One particular OTU (297), classified as *Thalassobium* sp., contributed 79 % of *Rhodobacteraceae* sequences on that day, but only 2–20 % in other samples. This peak corresponded to increased transcript accumulation from *Rhodobacteraceae* seen in the metatranscriptome analysis (Pfreundt et al., 2015) and a 4-fold increase in bacterial production on that day (Fig. 1d). This situation occurred the morning before the DIP fertilization and was accompanied by a relative increase in SAR86 and *Rhodospirillaceae* by 35 and 45 % to > 13 and 9.7 % of the 16S community, respectively. In addition, a 60 % drop in *Alteromonadaceae* down to 2 %, and a severe drop of *Synechococcus* from 20 to < 8 % of the 16S community were also observed (Fig. 3c, d, and f). While *Rhodobacteraceae* dropped to initial values similar to those in the lagoon on day 6 and contributed around 3 % until day 16, relative abundance of SAR11, dominated by the Surface 1 group, increased from 8 to 25 % of the 16S community on day 8 and outcompeted all other heterotrophic bacteria in M1 (Fig. 3c and d). SAR11 was replaced by SAR116, *Rhodospirillaceae* (mainly AEGEAN-169), and SAR86 two days later, on day 10, which constituted the three almost equally dominant groups until day 18 with 7 to 12 % of the 16S community each. On day 21, *Rhodobacteraceae* other than *Thalassobium* became the dominant heterotrophs in M1 and the lagoon (Figs. 3c and 4c).

Within alphaproteobacteria, SAR11 abundance dynamics were completely uncorrelated between M1 and the lagoon, whereas other groups were slightly positively correlated (Pearson correlation ∼ 0.5, Fig. S2c). Within gammaproteobacteria, *Alteromon-*

BGD
12, 20179–20222, 2015

adaceae and SAR86 together constituted between 75 % and almost 90 % (Fig. 3d) and whereas the former showed very similar dynamics between M1 and the lagoon waters, SAR86 did not (Fig. S2d). A second abundance peak of SAR86 occurred only in M1 on days 16 and 18 and coincided with similar peaks of the less abundant heterotrophic classes *Deferribacteres*, *Betaproteobacteria*, and *Cytophagia*. While SAR86 never decreased below 7.5 % in M1, these bacteria constituted below 6 % of the 16S community in the lagoon throughout P2 and dropped to 2.5 % on day 21.

Within *Flavobacteriia*, the dominant families exhibited highly correlated temporal dynamics in M1 and the lagoon and also between the different families (Fig. S2e). The *Flavobacteriaceae* family dominated, increasing more than three-fold between day 10 and 12, in the period of DIP consumption and coinciding with higher chl concentrations from day 12 onward (Figs. 1b and 2c). The maximum relative abundance of almost 15 % was reached in the lagoon on day 18 (Fig. 4e). In M1, *Flavobacteriaceae* constituted at most 9 %. Two other families, the NS7 and NS9 marine groups, had very low abundances until day 18, then increased afterwards.

3.2.3 Cyanobacteria

Synechococcus sp. (OTU-9) was the dominant OTU throughout the experiment in M1 and the lagoon, being almost an order of magnitude more abundant than the second ranked OTU at some time points. The steep drop of *Synechococcus* relative abundance on day 4 in M1, two days after the mesocosm closure, was equally seen in absolute counts by flow cytometry (from ~ 78 000 to ~ 44 000 cells mL^{-1}, Figs. 2a and 3f). At the same time in M1, *Prochlorococcus* gained in relative and absolute abundance reaching a maximum of 8 % of the 16S community on day 6, corresponding to ~ 16 000 and ~ 18 000 cells mL^{-1} on day 6 and 8, respectively (Figs. 2a and 3f). Variations in *Synechococcus* abundance correlated with changes in chl concentrations, except for days 2–5 with high *Synechococcus* cell counts but low chl concentrations (Figs. 1b and 2a). N_2-fixing cyanobacteria were generally one to two orders of magnitude less abundant than *Prochlorococcus* and *Synechococcus* and were in M1 most prevalent on day 2 and

BGD
12, 20179–20222, 2015

4, owing mainly to *Trichodesmium* with a maximum of 1.5 % of the 16S community on day 2 (Fig. 3f). After the DIP fertilization, *Trichodesmium* 16S tags dropped quickly by a factor of ten, leaving *Calothrix* as the most abundant detected diazotroph until day 12. Important to mention, the SILVA database used for 16S classification lists all *Richelia intracellularis* 16S sequences as descendants of the *Calothrix* node. This is discussed in Sect. 4. Candidatus *Atelocyanobacterium thalassa* (UCYN-A) constituted the third most abundant diazotroph until day 14. UCYN-A may be seen as a heterotrophic diazotroph, as it misses photosystem II, cannot fix CO_2 into biomass (Tripp et al., 2010), and lives in symbiosis with unicellular algae (Thompson et al., 2012). Between day 14 and 16, there was a steep increase of *Cyanothece* (UCYN-C), which had been increasing steadily after day 10, but at generally low levels. Nevertheless, UCYN-C was the most abundant diazotroph on day 16 (Fig. 3f). Heterotrophic diazotrophs like *Bradyrhizobium* and *Mesorhizobium* were, with a maximum of 0.01 % of the community for the former, not present in numbers anywhere close to those for N_2-fixing cyanobacteria. In the lagoon samples, the three dominant groups were the same, but with different dynamics. Notably, *Cyanothece* OTUs did not increase in abundance in the lagoon.

After day 4, the temporal evolution of relative (16S community) and absolute (flow cytometry) *Synechococcus* abundances in M1 diverged substantially (compare Figs. 3f and 2a). As *Synechococcus* and *Prochlorococcus* together constituted over 90 % of the cyanobacterial 16S community and thus up to 30 % of all 16S reads, changes in absolute cell counts for these groups can highly influence the temporal evolution of relative 16S data. To elude possible ambiguous interpretation of these data, we used the combined *Synechococcus* and *Prochlorococcus* cytometric counts to calculate a %16S/cell ratio for each sample (see Sect. 2.2). This ratio was then used to calculate absolute cell numbers from relative 16S abundance in M1 for all other groups investigated here (Fig. S3 in the Supplement). We assumed equal 16S gene copy numbers.

Interestingly, this approach revealed a steep increase (> 2-fold) of total non-photosynthetic cells (sum of all abundant classes except cyanobacteria and chloro-

BGD
12, 20179–20222, 2015

plasts per sample) from day 12 to day 16 in M1 that was not seen in flow cytometry counts of total heterotrophic bacteria (Fig. S3) but was accompanied by a moderate increase (50 %) in BP (Fig. 1d), supporting the former. Spearman rank correlation between BP and 16S-derived numbers for non-photosynthetic bacteria was 0.61 (0.73 when omitting day 21 with its prominent BP peak). N_2-fixation rates were also substantially higher throughout this period (days 12 to 16) than before and stayed high until the end of the experiment on day 23 (Fig. 1d). Preceding and overlapping this reaction of heterotrophs was a constant increase in *Synechococcus* from its minimum of $\sim 20\,000$ cells mL^{-1} on day 9 to maximally 103 000–104 000 cells mL^{-1} on day 19–20.

3.2.4 Temporal dynamics of the 16S community

Using all OTUs as a basis, we did unconstrained ordination of all samples on Bray–Curtis dissimilarities calculated from standardized relative abundances. Non-metric multidimensional scaling (NMDS) showed that inside M1 as well as in lagoon waters, the microbial communities defined three distinct clusters (Fig. 5a). Days 2–8, days 10–16, and days 18–21 (the last day 16S rRNA gene sequencing was done for) were grouped together and the clusters separated along the first MDS axis both in lagoon waters and in M1, whereas the locations lagoon waters and M1 (color coded in blue and orange, respectively) were also clearly separated along the second MDS axis. These clusters-in-time will be called *early*, *mid-time*, and *late* from here on and were time-delayed from the periods P0, P1, and P2 defined by biogeochemical parameters, production rates, and N_2 fixation (see Sect. 2.1). Thus, communities from M1 and the lagoon were clearly different from each other but followed a similar trajectory with time. When we separated the autotrophic community (547 OTUs) from the heterotrophic community (2981 OTUs, all OTUs other than cyanobacteria and chloroplasts) for ordination, it became evident that the heterotrophs showed a pattern very similar to the full community (Fig. 5b). The autotrophic community also clearly separated *early*, *mid-time*, and *late* phases from each other in M1 and the lagoon, but not as far, and separation by location (M1 vs. lagoon waters) only really became evident in the *late* phase (Fig. 5c).

BGD
12, 20179–20222, 2015

Analysis of variance (PERMANOVA) showed that indeed the community structures of the full OTU set, as well as both separate OTU sets, were significantly different between the three phases (predictor *time*) and were also different according to their origin, M1 or lagoon waters (predictor *location*, p values < 0.001, for autotrophs $p = 0.003$). Using the interaction of the predictor *location* with *time* additionally showed that *time* still had a significant effect after taking out the *location* effect but not the other way around. This shows that the effect of *time* was stronger and included the effect of *location*. Depth had no significant effect.

3.2.5 Effect of hydrological and biogeochemical parameters on the community structure of dominant OTUs

The 34 dominant OTUs (in terms of summed relative abundances of all samples) were subjected to constrained ordination within the frame of eight environmental variables (BP, PP, APA, Chl, POC, N_2 fixation, DIP, and temperature (T)), taking all samples from M1 and the lagoon from 1 and 12 m depth into account (Fig. 6). The sum of all unconstrained eigenvalues was 0.304, the sum of canonical eigenvalues 0.130. Thus, the amount of total variation in the species data that could be explained by the employed environmental variables was 43 % (permutation test, $p < 0.001$ after 999 permutations). The canonical axes F1 and F2 accounted for 50.5 and 22.3 % of this total explainable variance and 21.6 % and 9.5 % of the total variance, respectively. Both axes were significant and displayed strong species-environment correlations ($p < 0.001$ for both axes). Samples (location and time) were mainly separated along F1 with day 6 to 14 towards negative values and day 16 to 21 towards positive values. Interestingly, samples from M1 were separated further apart from each other than those from the lagoon. The main parameters separating samples and OTUs along the F1 axis were DIP, which was clearly higher in M1 samples following the DIP fertilization (days 6–10), and BP, Chl, and PP in opposition to DIP. Highly associated with BP and Chl were the *late* phase samples from M1 and lagoon, together with *Rhodobacteraceae* OTUs 1 and 37 and the flavobacterial NS4 marine group OTU 44, suggesting these directly profited

BGD
12, 20179–20222, 2015

from primary producers at the end of the experiment. Interestingly, another *Rhodobacteraceae* OTU (23) was tightly associated with N_2 fixation and with the OM60(NOR5) OTUs 2 and 18 from the *Halieaceae* family of gammaproteobacteria. Other gammaproteobacterial OTUs, *Alteromonas* OTU 13 and SAR86 OTUs 7 and 26, were positioned oppositely, closer to high DIP values, and together with all three SAR11 OTUs (43, 60, 2922), three of four SAR116 OTUs (16, 20, 34), the *Rickettsiales* group S25 (593) OTU 27 and Candidatus Actinomarina OTU 6 (*Actinobacteria*). Most tightly associated with high DIP concentrations was *Defluviicoccus* OTU 40 (*Rhodospirillaceae*). Also in the same quadrant, but forming a separate cluster, were MGII euryarchaea. Two more SAR86 OTUs (98, 1229) were separated from the rest and linked with *Prochlorococcus* and with the very early samples from day 2–4 in M1 and day 2–8 in the lagoon. One MGII and one SAR116 OTU (47 and 19) were also separated from the rest, possibly profiting from higher temperatures. More tightly linked with increasing temperatures and APA was the dominant flavobacterial OTU (*Sufflavibacter* OTU 67) in lagoon samples from days 16 to 21. Noteworthy, there was an opposition between the two dominant autotroph OTUs, *Synechococcus* (9) and *Prochlorococcus* (4), where the former was closely linked to the increase of PP and Chl at the end of the experiment. *Rhodospirillaceae* of the Aegean-169 group were positioned opposite to APA, T, and PP and close to *Prochlorococcus* and two chloroplast OTUs (3 and 1677), suggesting they might profit from these autotrophs specifically.

The quadrants resulting from this CCA nicely correspond to the clusters-in-time found through NMDS (Sect. 3.2.4), with few overlaps between quadrants: the bottom left corresponds to the *early* phase, the top left to the *mid-time* phase, and both right quadrants together to the *late* phase (compare Figs. 6 and 5).

BGD
12, 20179–20222, 2015

4 Discussion

4.1 *Synechococcus* as the most numerous primary producer

In the world's oceans, the unicellular cyanobacteria *Prochlorococcus* and *Synechococcus* constitute the most abundant marine picophytoplankton, amounting together up to 10^6 cells mL^{-1}, and are responsible for up to 50 % of the total CO_2 fixation in some regions (Liu et al., 1997; Li, 1994; Veldhuis et al., 1997). Previous studies (Zwirglmaier et al., 2008) showed that *Synechococcus* abundance is low in the oceanic oligotrophic gyres, reaching only 4×10^3 cells mL^{-1}, but up to 10^5 cells mL^{-1} in nutrient-rich upwelling regions (see also the data compilation in Flombaum et al., 2013). Therefore, the cell counts reported here for *Synechococcus* in the New Caledonian lagoon were with up to 10^5 cells mL^{-1} among the highest reported thus far for marine waters. In contrast, the maximum values for *Prochlorococcus* were relatively low. Several studies indicated that *Prochlorococcus* is adapted to ultra-oligotrophic conditions and is outcompeted by *Synechococcus* in waters of higher nutrient content, such as upwelling and coastal regions (Partensky et al., 1999a, b), which is consistent with the findings in this study (Leblanc et al., 2015). The *Synechococcus* group can be further delineated into several major clades with different ecophysiologies (Scanlan et al., 2009). Due to the insufficient phylogenetic resolution, this was not possible based on 16S rRNA gene sequencing. However, in the accompanying metatranscriptome analysis (Pfreundt et al., 2015), we found that the *Synechococcus* population was dominated by representatives of clade II and to a lower extent, clade IX, within the picophytoplankton subcluster 5.1A. These may correspond to the *Synechococcus* cells with low and high orange fluorescence, detected during cell sorting by flow cytometry (Van Wambeke et al., 2015), because the phycourobilin : phycoerythrobilin ratio differs between cultured representatives of these clades (Six et al., 2007) and phycourobilin may lead to high orange fluorescence. Recent analyses have suggested that the different frequencies of co-occurring *Synechococcus* ecotypes partition the ocean into four distinct regimes that can be distinguished by temperature, macronutrients and iron availability,

BGD
12, 20179–20222, 2015

suggesting clade II ecotypes are competitive in warmer, oligotrophic conditions (Sohm et al., 2015), which is consistent with the results of our metatranscriptomic analysis (Pfreundt et al., 2015). Measurements of BP and PP revealed that the organic matter produced by non-diazotrophic phytoplankton was the major carbon source fueling heterotrophic prokaryotes (Van Wambeke et al., 2015). Our community analysis identifies among these primary producers *Synechococcus* as the numerically most abundant contributor.

4.2 Effects of enclosure and DIP fertilization on the microbial community

Apart from investigating the effect of changing diazotroph communities on general community structure, we judged to which extent the enclosure and the DIP fertilization in the deployed large mesocosms changed community composition and development compared to the surrounding lagoon waters. Roughly, the 16S community composition partitioned the samples into three periods, an *early* period of DIP availability (including samples before the spike) until day 8, a *mid-time* period of DIP consumption, and a *late* period of Chl accumulation/P depletion starting with day 18. Remarkably, although we enriched the mesocosms with $\sim 0.8\,\mu M$ DIP and noticed a significant difference between the communities in M1 and in lagoon waters (Fig. 5a, separation along the second ordination axis, $p < 0.001$), the evolution of the both communities with time was mostly parallel, shown by their parallel separation along the first ordination axis. This indicates an overarching influence of abiotic factors acting on both locations equally, like temperature, which increased during the course of the study. Despite the parallel evolution of the full community (rare and abundant OTUs had similar weights in NMDS), community composition and dynamics of single abundant groups in M1 were different to those in the lagoon from the beginning. These differences first became evident with the drop in *Synechococcus* cell counts and 16S reads on days 2 to 4 (Figs. 2a and 3a). In this process, cyanophages might have played a role as suggested by the detected high gene expression from *Myoviridae* in M1 compared to the lagoon (Pfreundt et al., 2015). Based on the known host association of these T4-like phages (Frank et al.,

BGD
12, 20179–20222, 2015

2013; Ma et al., 2014; Sabehi et al., 2012), these were likely targeting *Synechococcus*. This event and its putative consequences on the availability of organic material coincided with diatoms sinking out of the water column in the mesocosms, roughly halving in numbers (Leblanc et al., 2015), and overlapped with DIP fertilization on day 4. Thus, it cannot be conclusively determined which had a higher influence on the community differences we observed in the *early* phase of the experiment, decaying phytoplankton or increased DIP concentrations. Van Wambeke et al. (Van Wambeke et al., 2015) showed that BP was not P-limited on day 4, suggesting that phytoplankton decay had the greater effect. Indeed, POC concentrations in M1, but not in the lagoon, increased from $\sim 10\,\mu mol\,L^{-1}$ on day 2 to $15\,\mu mol\,L^{-1}$ on day 4 (Berthelot et al., 2015).

We correlated the relative abundances in M1 and the Nouméa lagoon for all investigated phylogenetic groups (Fig. S2). This approach revealed alpha- and gammaproteobacteria as the least correlated classes between M1 and the lagoon. Investigating this aspect at higher taxonomic resolution showed that SAR11 and SAR86 temporal dynamics differed the most, suggesting that these groups were the most sensitive to changing nutrient sources. SAR11 was present at comparatively low numbers compared to other reports (Morris et al., 2002). We used filters with 0.45 µm pore size, so it cannot be excluded that SAR11 (average size 0.2 µm × 0.4 µm) and the even smaller Candidatus *Actinomarina* were lost at the beginning of filtering and retained when more cells were on the filter. Thus, we have possibly missed a substantial fraction of these groups in this study. Nevertheless, we can expect the loss rate to be very similar in all our samples, due to the following reasons: 16S and metatranscriptomics analyses were done from DNA and RNA isolated together from the same filter. Transcriptome abundances were tightly correlated (Pearson correlation 0.88 in M1, and 0.96 in the lagoon) between SAR86 and SAR11 (Pfreundt et al., 2015) over all samples. With different loss rates of SAR11 in different samples this correlation should not be possible.

SAR86, like SAR11, shows metabolic streamlining, but while SAR11 genomes contain putative genes for synthesis of most amino acids (Grote et al., 2012), a substantial fraction of natural SAR86 is probably auxotroph for Met, His and Arg (Dupont et al.,

BGD
12, 20179–20222, 2015

2012). Oppositely, SAR86 genomes encode a disproportionally high number of TonB dependent outer membrane receptors (TBDRs) that allow transport of > 600 Da molecules, including carbohydrates and lipids, combined with lipase genes and an expanded sugar utilization metabolism, whereas SAR11 genomes are not known to contain any TBDR genes and have strongly reduced sugar utilization capabilities (Dupont et al., 2012). In our accompanying metatranscriptome study, transcripts for TBDRs and phospholipase (days 14–16) from SAR86 were highly abundant, suggesting membrane lipids were used as an energy source (Pfreundt et al., 2015). Cultivation experiments of SAR11 representatives have shown their ability to utilize a wide variety of small organic molecules, including peptides, to generate energy (Tripp, 2013). The SAR11 subgroup Ia (surface 1) representative *Pelagibacter ubique* was able to supply one of its obligate required molecules (glycine) by glycolate (Carini et al., 2013), which is one of the main excretion by-products of phytoplankton and is assumed to be abundant in phytoplankton release. Finally, both SAR11 and SAR86 genomes contain proteorhodopsin genes, potentially providing an additional energy source, but the corresponding transcript levels were much higher in SAR11 than in SAR86 in this study (Pfreundt et al., 2015).

It appears striking that for both, SAR11 and SAR86, 16S abundance was not well correlated with the respective total transcript accumulation (Pfreundt et al., 2015), but that the two clades were correlated among each other both in transcript abundance and abundance of dominant OTUs. Dupont et al. (2012) hypothesized that, due to their different resource specializations, SAR11 and SAR86 compete only slightly for dissolved organic carbon (DOC), which would allow for their co-existence, albeit not explaining their correlation.

Interestingly, we saw niche partitioning among dominant SAR86 OTUs in constrained ordination (Fig. 6). The temporal variation of two OTUs was close to SAR11 and *Alteromonas* and of another two OTUs close to *Prochlorococcus*, suggesting different sources of DOC were utilized by these SAR86 subtypes. On 16S sequence level, pairwise alignments of these four SAR86 OTUs showed sequence identities between

BGD
12, 20179–20222, 2015

86.3 % (OTU 26 and 1229) and 94.9 % (OTU 7 and 98). Thus, those SAR86 OTUs sharing a niche were not more similar on 16S level than in between niches.

An aspect of special interest was to recognize community changes which could be attributed to the DIP fertilization and to possibly explain why. CCA suggested that the taxon profiting the most from DIP fertilization was *Defluviicoccus* (*Rhodospirillaceae*). Interestingly, *Defluviicoccus*-related bacteria were initially described from enhanced biological phosphorus removal systems (Maszenan et al., 2005; McIlroy and Seviour, 2009; Mielczarek et al., 2013). In such systems, *Defluviicoccus* are known as glycogen-accumulating bacteria, competing with polyphosphate accumulating organisms in enhanced biological phosphorus removal from waste water (Burow et al., 2007; McIlroy and Seviour, 2009; Wong et al., 2004; Wong and Liu, 2007). It is therefore interesting that in constrained ordination, the dominant *Defluviicoccus* OTU (40) was associated with DIP for M1 samples on days 6, 8 and 10, immediately following the phosphorus fertilization (Fig. 6). While not showing this apparent reaction to DIP, this OTU had similar abundances also in the Nouméa lagoon. There are only few studies reporting *Defluviicoccus*-related bacteria in marine samples, and if so, these were associated with marine invertebrates (Enomoto et al., 2012; Fan et al., 2013). Based on our data it is likely that there was a minor population of *Defluviicoccus*-related bacteria that could benefit from the addition of fresh phosphorus in M1. Note however, that this OTU was only 83 % identical to *Defluviicoccus vanus* 16S, but 99 % identical to environmental sequences that, according to SILVA taxonomy for SSU release 119 and 123, are leaves of the same node as *D. vanus* and were thus classified as *Defluviicoccus* (name of the node). Therefore, additional work towards the more precise characterization of these *Defluviicoccus*-related bacteria is required.

4.3 Effects of DIP depletion at the end of the experiment

Some aspects of the taxonomic succession after day 13, when DIP was mainly depleted, can be related to the strategies used for adaptation to P limitation. Among autotrophs, the main trend observed in M1 and the lagoon waters was the opposition

BGD
12, 20179–20222, 2015

of *Prochlorococcus* and *Synechococcus* with *Synechococcus* reaching higher abundances in M1 at the end of the experiment compared to the beginning, when DIP was comparatively low. Both expressed alkaline phosphatase (AP) mainly two days after their respective 16S abundance peak (Pfreundt et al., 2015), suggesting that the increase in cell numbers led to a higher phosphorous demand that was subsequently adapted to. Incorporation of sulfolipids instead of phospholipids into membrane lipids is an ecological strategy developed by cyanobacteria for an advantage in P deficient environments (Van Mooy et al., 2006, 2009). The ability to synthetize sulphoquinovosyldiacylgycerol in place of phosphatidylglycerol in P-limited cultures can save 5 to 43 % of total cellular phosphorus demand and is highly variable according to the strain tested (Van Mooy et al., 2009). *SqdB*, a gene encoding a sulfolipid synthesis protein, was mainly transcribed by *Synechococcus* and less by *Prochlorococcus* (Pfreundt et al., 2015) and corresponded to their changes in 16S abundance. In the North Atlantic Ocean, *Synechococcus* are also good competitors with *Prochlorococcus* for DIP and ATP uptake (Michelou et al., 2011). A variety of heterotrophs expressed AP mainly after day 10, possibly to the benefit of other populations. Indeed, metagenomic analyses showed that 59 % of marine bacterial APs are extracellular, periplasmic or located at the outer membrane (Luo et al., 2009). Possibly, DIP release through extracellular APA may provide P to neighboring cells that cannot synthesize this enzyme, and such effects could possibly be emphasized in macro-aggregate gels seen during P2 (Berman-Frank et al., 2015).

4.4 Possible functional roles of bacterial subcommunities in the degradation of organic matter

The concerted increase of *Cytophagia* and *Flavobacteriia* towards the end of the experiment is a recurrent feature seen in older studies based on plateable strains (Fukami et al., 1981b; Painting et al., 1989), and in molecular studies allowing access to the uncultivable community (Teeling et al., 2012). Both *Cytophagia* and *Flavobacteriia* profit from phytoplankton blooms and have often been found in marine snow (DeLong et al.,

BGD
12, 20179–20222, 2015

1993; Fontanez et al., 2015; Teeling et al., 2012). Members of the *Flavobacteriia* are known to degrade organic matter, some even specializing on algal-derived organic matter (Bauer et al., 2006; Bowman, 2006). In the lagoon, members of the *Flavobacteriaceae* reached even higher relative abundances than in M1. The occurrence of different *Flavobacteriaceae* phylotypes seems to depend on the nature of the dominant phytoplankton species (Pinhassi et al., 2004). Information retrieved from analysis of cultured representatives show a high capacity to degrade high molecular weight molecules, which is in line with the high ectoenzymatic activities generally associated at the end of blooms (Chróst, 1992; Riemann et al., 2000). The quality of organic matter issued from specific phytoplankton detritus influences bacterial community succession, and while the potential for polymer degradation appears to be widespread among different phyla it is restricted to some very specialized species (Landa et al., 2014; Murray et al., 2007). Our data indicate that both in M1 and the lagoon, there were organic components available favoring their growth, most pronounced during P2.

Our data further indicate that *Rhodobacteraceae*, when abundant, assimilate much more organic matter than other heterotrophs seen in this study, as dynamics in BP were closely linked to this group. This was not only shown by CCA (Fig. 5) but is also evident from directly comparing BP (Van Wambeke et al., 2015) to *Rhodobacteraceae* 16S reads. Both striking BP peaks on day 4 and day 21 in M1 correspond to concomitant peaks in *Rhodobacteraceae* 16S, while no other heterotrophic groups showed these peaks. *Rhodobacteraceae* are considered ecological generalists, with large gene inventories, but they cannot be easily condensed in an ecologically differentiated cluster (Newton et al., 2010). *Roseobacter*, a common marine member of the *Rhodobacteraceae*, have a variety of metabolic pathways that facilitate interaction and attachment with phytoplankton detritus or give them advantages among other bacteria. They can produce quorum sensing molecules, vitamins and antimicrobial compounds (Buchan et al., 2014). CCA showed two dominating *Rhodobacteriaceae* OTUs linked with chl concentrations (Fig. 5), which argues for their ability to access phytoplankton detritus, while one OTU was closely linked with N_2 fixation. Notably, none of these three OTUs

BGD
12, 20179–20222, 2015

represented the *Thalassobius* sp. OTU that was responsible for the *Rhodobacteraceae* peak on day 4.

4.5 The diazotroph community and its impact on the heterotroph community structure

Diazotroph community structure (Figs. 3f and 4f) probably changed in M1 due to DIP fertilization and reduced turbulence, with *Cyanothece*-like cells profiting and forming large aggregates during P2 (Bonnet et al., 2015a). Our 16S based diazotroph abundances compare reasonably well with those found by quantitative PCR of the *nifH* gene (Turk-Kubo et al., 2015), if we assume that those 16S reads classified as *Calothrix* are indeed mostly *Richelia* (Het-1). The SILVA database positions *Richelia* below the *Calothrix* node, and the metatranscriptome data published in this issue show a substantial *Richelia* read fraction and only little *Calothrix* (Pfreundt et al., 2015), supporting this assumption. Further, UCYN-C *nifH* gene abundance was at maximum 100 copies mL^{-1} in M1 (Turk-Kubo et al., 2015), which matches well the maximal 500 cells mL^{-1} that we calculated from relative 16S values for *Cyanothece* using flow cytometry counts of *Synechococcus* and *Prochlorococcus* (Fig. S3f). Note that there are also non-diazotrophic *Cyanothece* representatives. This is remarkable given the different methods used to produce these numbers.

The higher *Trichodesmium* abundance inside M1 after its deployment might be attributed to entrapment of filaments that were not present in the lagoon anymore when the sampling started, likely due to high tide currents. The reduction in the number of 16S tags belonging to *Trichodesmium* following the DIP fertilization on the evening of day 4 was unexpected. To the contrary, the combined effects of reduced turbulence and P limitation was thought to trigger a *Trichodesmium* bloom. However, a *Trichodesmium* bloom was observed at the end of the VAHINE experiment in the lagoon (Spungin et al., 2015), demonstrating that the small numbers of existing filaments were competent to build up blooms rapidly. While we did see cyanophage gene expression in M1 in the accompanying metatranscriptome study (Pfreundt et al., 2015), the known host ranges

BGD
12, 20179–20222, 2015

of those phages suggest that they rather would act on *Synechococcus*, excluding viral lysis as the reason for the *Trichodesmium* decline. Thus, there were likely other factors involved that deserve further investigation. *Trichodesmium* has comparatively low growth rates (Turk-Kubo et al., 2015), so enhanced competition after DIP fertilization might be such a factor.

Average N_2 fixation rates of $27.3 \pm 1.0\,\mathrm{nmol\,N\,L^{-1}\,d^{-1}}$ were measured inside the mesocosms during P2 (days 15–23), and with $69.7\,\mathrm{nmol\,N\,L^{-1}\,d^{-1}}$ very high maximum rates were reached in M1 between days 18 and 21. A short-term experiment performed by Bonnet et al. (2015a) indicated that DDN was efficiently transferred to non-diazotrophic microbial communities during P2: after 24 h, 16 ± 6 % of the fixed N_2 was released in the dissolved nitrogen pool and 18 ± 4 % was transferred to non-diazotrophic picoplankton. We show that in terms of relative abundance, SAR86, *Deferribacteres*, *Deltaproteobacteria*, *Cytophagia*, and *Flavobacteriaceae* increased during this period (Fig. 3). In terms of pseudo-absolute abundances, calculated from 16S abundances employing the cytometry cell counts of *Synechococcus* and *Prochlorococcus*, it became clear that indeed almost all heterotrophic groups analyzed here (> 0.5 % relative abundance) increased during this period (Fig. S3). Another publication in this issue showed that BP was always stimulated after short-term ammonium plus nitrate enrichments on day 4 and 20 (Van Wambeke et al., 2015). This finding speaks for a positive effect of released DDN on heterotrophic growth during P2, but effects through phytoplankton growth and decay probably also played a role. Indeed, nitrogen coming from N_2 fixation alone was not sufficient to sustain BP (Van Wambeke et al., 2015). Constrained ordination showed that generally, temporal variation of dominant *Rhodobacteraceae*, *Halieaceae* (OM60(NOR5), in SILVA release 119 within the *Alteromonadaceae*), and *Flavobacteriia* could be partially be explained with changes in N_2 fixation, whereas variation in other alphaproteobacteria (mainly SAR11, SAR116, and *Rhodospirillaceae*), SAR86, euryarchaea, and *Alteromonas* abundances were not explainable by N_2 fixation (Fig. 6), indicating the involvement of additional factors. However, it appears very clear that the shift within the diazotroph community from the dom-

BGD
12, 20179–20222, 2015

inant diazotrophs *Richelia* and *Trichodesmium* to UCYN-C after day 14, together with very high N_2 fixation rates (Bonnet et al., 2015a), led to an increase in abundance of almost all heterotrophic groups investigated here, consistent with N limitation of BP (Van Wambeke et al., 2015).

5 Conclusions

We show that despite their large size ($> 50\,m^3$), the VAHINE mesocosms led to significant changes in the microbial community structure, probably initiated by decay of *Synechococcus* and diatoms (Leblanc et al., 2015), albeit not exhibiting a typical bottle effect with a copiotroph-dominated community. Interestingly, the accompanying metatranscriptome study for M1 showed gene expression from cyanophages, which might have contributed to *Synechococcus* decay. Fertilization with 0.8 µM DIP on day 4 did not have directly observable effects on the overall community, as samples from before and four days after fertilization clustered together, but likely influenced development of individual populations, like *Defluviicoccus*-related bacteria or UCYN-C diazotrophs. The latter increased after day 10 only in the mesocosms, and were probably limited by temperature before that (Turk-Kubo et al., 2015). The shift of the dominant diazotroph from *Richelia* and *Trichodesmium* to UCYN-C after day 14 (Turk-Kubo et al., 2015), together with extremely high N_2 fixation rates (Bonnet et al., 2015a), led to an increase in abundance of almost all heterotrophic groups investigated here, consistent with N-limited BP (Van Wambeke et al., 2015).

Linked with the observation of tight correlation between SAR11 and SAR86 transcription during a diel cycle (Aylward et al., 2015) and over three weeks (Pfreundt et al., 2015), we show that the temporal dynamics of individual OTUs of these clades over three weeks can be explained by very similar combinations of environmental variables. With the results of this work we present for the first time in this ecosystem an in-depth analysis of the prokaryotic diversity and community structure and of their changes over time with a focus on diazotrophic organisms. We correlate the prokaryotic community

BGD
12, 20179–20222, 2015

structure with effects of DIP fertilization, of enclosure vs. open waters in the lagoon, and with the fate of DDN and DOC. The determined microbial diversity was very high, and we provide evidence for previously unknown niche partitioning, e.g., among dominant SAR86 OTUs. These results suggest a plethora of still unknown metabolic and regulatory interactions to occur within these marine microbial communities that are worth to be explored further.

Data availability

All raw sequencing data can be downloaded from NCBI's BioProject database under the accession number BioProject PRJNA304389.

The Supplement related to this article is available online at doi:10.5194/bgd-12-20179-2015-supplement.

Author contributions. S. Bonnet is the chief scientist responsible of the VAHINE program, she designed and executed the experiment in mesocosms and measured N_2 fixation. F. Van Wambeke sampled for and prepared Figs. 1 and 6, W. R. Hess and U. Pfreundt took samples, U. Pfreundt prepared and analyzed 16S rRNA gene amplicons and prepared all other figures, U. Pfreundt, F. Van Wambeke and W. R. Hess drafted the manuscript, all authors reviewed the manuscript.

Acknowledgements. Funding for this research was provided by the Agence Nationale de la Recherche (ANR starting grant VAHINE ANR-13-JS06-0002), INSU-LEFE-CYBER program, GOPS, IRD and M.I.O. The participation of UP and WRH was supported by the German-Israeli Research Foundation (GIF), project number 1133-13.8/2011 and the MiSeq-based microbial community analysis by the EU project MaCuMBA (Marine Microorganisms: Cultivation Methods for Improving their Biotechnological Applications; grant agreement no: 311975) to WRH. The authors thank the captain and crew of the R/V *Alis*. We acknowledge the SEOH divers service from the IRD research center of Nouméa (E. Folcher, B. Bourgeois and A. Renaud) and from the Observatoire Océanologique de Villefranche-sur-mer (OOV, J. M. Grisoni) as well

BGD
12, 20179–20222, 2015

as the technical service of the IRD research center of Nouméa for their helpful technical support. C. Guieu, F. Louis and J. M. Grisoni (Laboratoire d'Océanographie de Villefranche (LOV) and Observatoire céalonologique de Villefranche-sur-mer (OOV)) are warmly thanked for the mesocosms design and their useful advice for deployment, Anne Desnues and Dina Spungin for help in sampling, T. Moutin, M. Rodier and H. Berthelot for providing their data and Craig Nelson from the University of Hawaii at Manoa for advice on NMDS analysis. We are grateful to the Regional Flow Cytometry Platform for Microbiology (PRECYM) of the Mediterranean Institute of Oceanography (MIO) for the flow cytometry analyses.

References

Alonso-Sáez, L. and Gasol, J. M.: Seasonal variations in the contributions of different bacterial groups to the uptake of low-molecular-weight compounds in northwestern Mediterranean coastal waters, Appl. Environ. Microb., 73, 3528–3535, doi:10.1128/AEM.02627-06, 2007.

Aylward, F. O., Eppley, J. M., Smith, J. M., Chavez, F. P., Scholin, C. A., and DeLong, E. F.: Microbial community transcriptional networks are conserved in three domains at ocean basin scales, P. Natl. Acad. Sci. USA, 112, 5443–5448, doi:10.1073/pnas.1502883112, 2015.

Bauer, M., Kube, M., Teeling, H., Richter, M., Lombardot, T., Allers, E., Würdemann, C. A., Quast, C., Kuhl, H., Knaust, F., Woebken, D., Bischof, K., Mussmann, M., Choudhuri, J. V., Meyer, F., Reinhardt, R., Amann, R. I., and Glöckner, F. O.: Whole genome analysis of the marine Bacteroidetes "Gramella forsetii" reveals adaptations to degradation of polymeric organic matter, Environ. Microbiol., 8, 2201–2213, doi:10.1111/j.1462-2920.2006.01152.x, 2006.

Beier, P. and de Albuquerque, F. S.: Environmental diversity as a surrogate for species representation, Conserv. Biol., 29, 1401–1410, doi:10.1111/cobi.12495, 2015.

Berman-Frank, I., Spungin, D., Rahav, E., Van Wambeke, F., Turk-Kubo, K., and Moutin, T.: Dynamics of Transparent Exopolymer Particles (TEP) during the VAHINE mesocosm experiment in the New Caledonia lagoon, Biogeosciences Discuss., submitted, 2015.

Berthelot, H., Moutin, T., L'Helguen, S., Leblanc, K., Hélias, S., Grosso, O., Leblond, N., Charrière, B., and Bonnet, S.: Dinitrogen fixation and dissolved organic nitrogen fueled primary production and particulate export during the VAHINE mesocosm experiment (New Caledonia lagoon), Biogeosciences, 12, 4099–4112, doi:10.5194/bg-12-4099-2015, 2015.

BGD
12, 20179–20222, 2015

Biddanda, B. and Pomeroy, L.: Microbial aggregation and degradation of phytoplankton-derived detritus in seawater. I. Microbial succession, Mar. Ecol.-Prog. Ser., 42, 79–88, doi:10.3354/meps042079, 1988.

Biegala, I. C. and Raimbault, P.: High abundance of diazotrophic picocyanobacteria (< 3 µm) in a Southwest Pacific coral lagoon, Aquat. Microb. Ecol., 51, 45–53, doi:10.3354/ame01185, 2008.

Bonnet, S., Berthelot, H., Turk-Kubo, K., Fawcett, S., Rahav, E., l'Helguen, S., and Berman-Frank, I.: Dynamics of N2 fixation and fate of diazotroph-derived nitrogen in a low nutrient low chlorophyll ecosystem: results from the VAHINE mesocosm experiment (New Caledonia), Biogeosciences Discuss., 12, 19579–19626, doi:10.5194/bgd-12-19579-2015, 2015a.

Bonnet, S., Moutin, T., Rodier, M., Grisoni, J. M., Louis, F., Folcher, E., Bourgeois, B., Boré, J. M., and Renaud, A.: Introduction to the project VAHINE: VAriability of vertical and tropHIc transfer of fixed N_2 in the south wEst Pacific, Biogeosciences Discuss., submitted, 2015b.

Bowman, J. P.: The Marine Clade of the Family Flavobacteriaceae: the Genera Aequorivita, Arenibacter, Cellulophaga, Croceibacter, Formosa, Gelidibacter, Gillisia, Maribacter, Mesonia, Muricauda, Polaribacter, Psychroflexus, Psychroserpens, Robiginitalea, Salegentibacter, Tenacibaculum, Ulvibacter, Vitellibacter and Zobellia, in: The Prokaryotes, Springer, New York, USA, 677–694, available at: http://link.springer.com/referenceworkentry/10.1007/0-387-30747-8_26, last access: 2 December 2015, 2006.

Buchan, A., LeCleir, G. R., Gulvik, C. A., and González, J. M.: Master recyclers: features and functions of bacteria associated with phytoplankton blooms, Nat. Rev. Microbiol., 12, 686–698, doi:10.1038/nrmicro3326, 2014.

Burow, L. C., Kong, Y., Nielsen, J. L., Blackall, L. L., and Nielsen, P. H.: Abundance and ecophysiology of Defluviicoccus spp., glycogen-accumulating organisms in full-scale wastewater treatment processes, Microbiology+, 153, 178–185, doi:10.1099/mic.0.2006/001032-0, 2007.

Carini, P., Steindler, L., Beszteri, S., and Giovannoni, S. J.: Nutrient requirements for growth of the extreme oligotroph "Candidatus Pelagibacter ubique" HTCC1062 on a defined medium, ISME J., 7, 592–602, doi:10.1038/ismej.2012.122, 2013.

Chróst, R. J.: Significance of bacterial ectoenzymes in aquatic environments, Hydrobiologia, 243/244, 61–70, 1992.

BGD
12, 20179–20222, 2015

DeLong, E. F., Franks, D. G., and Alldredge, A. L.: Phylogenetic diversity of aggregate-attached vs. free-living marine bacterial assemblages, Limnol. Oceanogr., 38, 924–934, doi:10.4319/lo.1993.38.5.0924, 1993.

Dupont, C. L., Rusch, D. B., Yooseph, S., Lombardo, M.-J., Alexander Richter, R., Valas, R., Novotny, M., Yee-Greenbaum, J., Selengut, J. D., Haft, D. H., Halpern, A. L., Lasken, R. S., Nealson, K., Friedman, R., and Craig Venter, J.: Genomic insights to SAR86, an abundant and uncultivated marine bacterial lineage, ISME J., 6, 1186–1199, doi:10.1038/ismej.2011.189, 2012.

Edgar, R. C.: UPARSE: highly accurate OTU sequences from microbial amplicon reads, Nat. Methods, 10, 996–998, doi:10.1038/nmeth.2604, 2013.

Enomoto, M., Nakagawa, S., and Sawabe, T.: Microbial communities associated with holothurians: presence of unique bacteria in the coelomic fluid, Microbes. Environ., 27, 300–305, 2012.

Fan, L., Liu, M., Simister, R., Webster, N. S., and Thomas, T.: Marine microbial symbiosis heats up: the phylogenetic and functional response of a sponge holobiont to thermal stress, ISME J., 7, 991–1002, doi:10.1038/ismej.2012.165, 2013.

Flombaum, P., Gallegos, J. L., Gordillo, R. A., Rincón, J., Zabala, L. L., Jiao, N., Karl, D. M., Li, W. K. W., Lomas, M. W., Veneziano, D., Vera, C. S., Vrugt, J. A., and Martiny, A. C.: Present and future global distributions of the marine Cyanobacteria Prochlorococcus and Synechococcus, P. Natl. Acad. Sci. USA, 110, 9824–9829, doi:10.1073/pnas.1307701110, 2013.

Fontanez, K. M., Eppley, J. M., Samo, T. J., Karl, D. M., and DeLong, E. F.: Microbial community structure and function on sinking particles in the North Pacific Subtropical Gyre, Front. Microbiol., 6, 469, doi:10.3389/fmicb.2015.00469, 2015.

Frank, J. A., Lorimer, D., Youle, M., Witte, P., Craig, T., Abendroth, J., Rohwer, F., Edwards, R. A., Segall, A. M., and Burgin, A. B.: Structure and function of a cyanophage-encoded peptide deformylase, ISME J., 7, 1150–1160, doi:10.1038/ismej.2013.4, 2013.

Fukami, K., Simidu, U., and Taga, N.: A microbiological study on the decline process of a phyto plankton bloom in Aburatsubo Inlet, Kanagawa, Japan, B. Plankton Soc. Jpn., 28, 33–41, 1981a.

Fukami, K., Simidu, U., and Taga, N.: Fluctuation of the communities of heterotrophic bacteria during the decomposition process of phytoplankton, J. Exp. Mar. Biol. Ecol., 55(2–3), 171–184, doi:10.1016/0022-0981(81)90110-6, 1981b.

BGD
12, 20179–20222, 2015

Garcia, N., Raimbault, P., and Sandroni, V.: Seasonal nitrogen fixation and primary production in the Southwest Pacific: nanoplankton diazotrophy and transfer of nitrogen to picoplankton organisms, Mar. Ecol.-Prog. Ser., 343, 25–33, doi:10.3354/meps06882, 2007.

Grote, J., Thrash, J. C., Huggett, M. J., Landry, Z. C., Carini, P., Giovannoni, S. J., and Rappé, M. S.: Streamlining and core genome conservation among highly divergent members of the SAR11 clade, mBio, 3, e00252-12, doi:10.1128/mBio.00252-12, 2012.

Klindworth, A., Pruesse, E., Schweer, T., Peplies, J., Quast, C., Horn, M., and Glöckner, F. O.: Evaluation of general 16S ribosomal RNA gene PCR primers for classical and next-generation sequencing-based diversity studies, Nucleic Acids Res., 41, e1, doi:10.1093/nar/gks808, 2013.

Landa, M., Cottrell, M. T., Kirchman, D. L., Kaiser, K., Medeiros, P. M., Tremblay, L., Batailler, N., Caparros, J., Catala, P., Escoubeyrou, K., Oriol, L., Blain, S., and Obernosterer, I.: Phylogenetic and structural response of heterotrophic bacteria to dissolved organic matter of different chemical composition in a continuous culture study, Environ. Microbiol., 16, 1668–1681, doi:10.1111/1462-2920.12242, 2014.

Lebaron, P., Servais, P., Troussellier, M., Courties, C., Muyzer, G., Bernard, L., Schäfer, H., Pukall, R., Stackebrandt, E., Guindulain, T., and Vives-Rego, J.: Microbial community dynamics in Mediterranean nutrient-enriched seawater mesocosms: changes in abundances, activity and composition, FEMS Microbiol. Ecol., 34, 255–266, 2001.

Leblanc, K., Cornet, V., Caffin, M., Rodier, M., Desnues, A., Berthelot, H., Turk-Kubo, K. A., and Heliou, J.: Phytoplankton community structure in the VAHINE mesocosm experiment, Biogeosciences Discuss., submitted, 2015.

Li, W. K. W.: Primary production of prochlorophytes, cyanobacteria, and eucaryotic ultraphytoplankton: measurements from flow cytometric sorting, Limnol. Oceanogr., 39, 169–175, 1994.

Liu, H., Nolla, H. A., and Campbell, L.: Prochlorococcus growth rate and contribution to primary production in the equatorial and subtropical North Pacific Ocean, Aquat. Microb. Ecol., 12, 39–47, doi:10.3354/ame012039, 1997.

Luo, H., Benner, R., Long, R. A., and Hu, J.: Subcellular localization of marine bacterial alkaline phosphatases, P. Natl. Acad. Sci. USA, 106(50), 21219–21223, doi:10.1073/pnas.0907586106, 2009.

Luo, Y.-W., Doney, S. C., Anderson, L. A., Benavides, M., Berman-Frank, I., Bode, A., Bonnet, S., Boström, K. H., Böttjer, D., Capone, D. G., Carpenter, E. J., Chen, Y. L., Church, M. J.,

BGD
12, 20179–20222, 2015

Dore, J. E., Falcón, L. I., Fernández, A., Foster, R. A., Furuya, K., Gómez, F., Gundersen, K., Hynes, A. M., Karl, D. M., Kitajima, S., Langlois, R. J., LaRoche, J., Letelier, R. M., Marañón, E., McGillicuddy Jr., D. J., Moisander, P. H., Moore, C. M., Mouriño-Carballido, B., Mulholland, M. R., Needoba, J. A., Orcutt, K. M., Poulton, A. J., Rahav, E., Raimbault, P., Rees, A. P., Riemann, L., Shiozaki, T., Subramaniam, A., Tyrrell, T., Turk-Kubo, K. A., Varela, M., Villareal, T. A., Webb, E. A., White, A. E., Wu, J., and Zehr, J. P.: Database of diazotrophs in global ocean: abundance, biomass and nitrogen fixation rates, Earth Syst. Sci. Data, 4, 47–73, doi:10.5194/essd-4-47-2012, 2012.

Ma, Y., Allen, L. Z., and Palenik, B.: Diversity and genome dynamics of marine cyanophages using metagenomic analyses, Environ. Microbiol. Rep., 6, 583–594, 2014.

Maszenan, A. M., Seviour, R. J., Patel, B. K. C., Janssen, P. H., and Wanner, J.: Defluvicoccus vanus gen. nov., sp. nov., a novel Gram-negative coccus/coccobacillus in the "Alphaproteobacteria" from activated sludge, Int. J. Syst. Evol. Micr., 55, 2105–2111, doi:10.1099/ijs.0.02332-0, 2005.

McIlroy, S. and Seviour, R. J.: Elucidating further phylogenetic diversity among the Defluviicoccus-related glycogen-accumulating organisms in activated sludge, Environ. Microbiol. Rep., 1, 563–568, doi:10.1111/j.1758-2229.2009.00082.x, 2009.

Michelou, V. K., Lomas, M. W., and Kirchman, D. L.: Phosphate and adenosine-5'-triphosphate uptake by cyanobacteria and heterotrophic bacteria in the Sargasso Sea, Limnol. Oceanogr., 56, 323–332, doi:10.4319/lo.2011.56.1.0323, 2011.

Mielczarek, A. T., Nguyen, H. T. T., Nielsen, J. L., and Nielsen, P. H.: Population dynamics of bacteria involved in enhanced biological phosphorus removal in Danish wastewater treatment plants, Water Res., 47, 1529–1544, doi:10.1016/j.watres.2012.12.003, 2013.

Moisander, P. H., Beinart, R. A., Hewson, I., White, A. E., Johnson, K. S., Carlson, C. A., Montoya, J. P., and Zehr, J. P.: Unicellular cyanobacterial distributions broaden the oceanic N_2 fixation domain, Science, 327, 1512–1514, doi:10.1126/science.1185468, 2010.

Morris, R. M., Rappé, M. S., Connon, S. A., Vergin, K. L., Siebold, W. A., Carlson, C. A., and Giovannoni, S. J.: SAR11 clade dominates ocean surface bacterioplankton communities, Nature, 420, 806–810, doi:10.1038/nature01240, 2002.

Moutin, T., Karl, D. M., Duhamel, S., Rimmelin, P., Raimbault, P., Van Mooy, B. A. S., and Claustre, H.: Phosphate availability and the ultimate control of new nitrogen input by nitrogen fixation in the tropical Pacific Ocean, Biogeosciences Discuss., 4, 2407–2440, doi:10.5194/bgd-4-2407-2007, 2007.

BGD
12, 20179–20222, 2015

Murray, A. E., Arnosti, C., Rocha, C. L. D. L., Grossart, H., and Passow, U.: Microbial dynamics in autotrophic and heterotrophic seawater mesocosms. II. Bacterioplankton community structure and hydrolytic enzyme activities, Aquat. Microb. Ecol., 49, 123–141, doi:10.3354/ame01139, 2007.

Nagata, T.: Production mechanisms of dissolved organic matter, in Microbial Ecology of the Oceans, edited by: Kirchman, D. L., Wiley, Lissabon, 121–152, 2000.

Oksanen, J., Blanchet, F. G., Kindt, R., Legendre, P., Minchin, P. R., O'Hara, R. B., Simpson, G. L., Solymos, P., Stevens, M. H. H., and Wagner, H.: vegan: Community Ecology Package, available at: http://CRAN.R-project.org/package=vegan, last access: May 2015.

Painting, S. J., Lucas, M. I., and Muir, D. G.: Fluctuations in heterotrophic bacterial community structure, activity and production in response to development and decay of phytoplankton in a microcosm., Mar. Ecol.-Prog. Ser., 53, 129–141, 1989.

Partensky, F., Blanchot, J., and Vaulot, D.: Differential distribution and ecology of Prochlorococcus and Synechococcus in oceanic waters: a review, Bull. Inst. Océan., 19, 457–475, 1999a.

Partensky, F., Hess, W. R., and Vaulot, D.: Prochlorococcus, a marine photosynthetic prokaryote of global significance, Microbiol. Mol. Biol. R., 63, 106–127, 1999b.

Pfreundt, U., Spungin, D., Bonnet, S., Berman-Frank, I., and Hess, W. R.: Global analysis of gene expression dynamics within the marine microbial community during the VAHINE mesocosm experiment in the South West Pacific, Biogeosciences Discuss., submitted, 2015.

Pinhassi, J., Sala, M. M., Havskum, H., Peters, F., Guadayol, O., Malits, A., and Marrasé, C.: Changes in bacterioplankton composition under different phytoplankton regimens, Appl. Environ. Microb., 70, 6753–6766, doi:10.1128/AEM.70.11.6753-6766.2004, 2004.

Pinto, F. L., Thapper, A., Sontheim, W., and Lindblad, P.: Analysis of current and alternative phenol based RNA extraction methodologies for cyanobacteria, BMC Mol. Biol., 10, 79, doi:10.1186/1471-2199-10-79, 2009.

Quast, C., Pruesse, E., Yilmaz, P., Gerken, J., Schweer, T., Yarza, P., Peplies, J., and Glöckner, F. O.: The SILVA ribosomal RNA gene database project: improved data processing and web-based tools, Nucleic Acids Res., 41, D590–596, doi:10.1093/nar/gks1219, 2013.

Riemann, L., Steward, G. F., and Azam, F.: Dynamics of bacterial community composition and activity during a mesocosm diatom bloom, Appl. Environ. Microb., 66, 578–587, 2000.

Rognes, T., Mahé, F., Flouri, T., McDonald, D., and Schloss, P.: vsearch: VSEARCH 1.4.0, doi:10.5281/zenodo.31443, 2015.

BGD
12, 20179–20222, 2015

Sabehi, G., Shaulov, L., Silver, D. H., Yanai, I., Harel, A., and Lindell, D.: A novel lineage of myoviruses infecting cyanobacteria is widespread in the oceans, P. Natl. Acad. Sci. USA, 109, 2037–2042, doi:10.1073/pnas.1115467109, 2012.

Scanlan, D. J., Ostrowski, M., Mazard, S., Dufresne, A., Garczarek, L., Hess, W. R., Post, A. F., Hagemann, M., Paulsen, I., and Partensky, F.: Ecological genomics of marine picocyanobacteria, Microbiol. Mol. Biol. R., 73, 249–299, doi:10.1128/MMBR.00035-08, 2009.

Six, C., Thomas, J.-C., Garczarek, L., Ostrowski, M., Dufresne, A., Blot, N., Scanlan, D. J., and Partensky, F.: Diversity and evolution of phycobilisomes in marine Synechococcus spp.: a comparative genomics study, Genome Biol., 8, R259, doi:10.1186/gb-2007-8-12-r259, 2007.

Sohm, J. A., Ahlgren, N. A., Thomson, Z. J., Williams, C., Moffett, J. W., Saito, M. A., Webb, E. A., and Rocap, G.: Co-occurring Synechococcus ecotypes occupy four major oceanic regimes defined by temperature, macronutrients and iron, ISME J., doi:10.1038/ismej.2015.115, 2015.

Spungin, D., Pfreundt, U., Berthelot, H., Bonnet, S., Al-Roumi, D., Natale, F., Hess, W. R., Bidle, K. D., and Berman-Frank, I.: Mechanisms of Trichodesmium bloom demise within the New Caledonia Lagoon during the VAHINE mesocosm e xperiment, Biogeosciences Discuss., submitted, 2015.

Teeling, H., Fuchs, B. M., Becher, D., Klockow, C., Gardebrecht, A., Bennke, C. M., Kassabgy, M., Huang, S., Mann, A. J., Waldmann, J., Weber, M., Klindworth, A., Otto, A., Lange, J., Bernhardt, J., Reinsch, C., Hecker, M., Peplies, J., Bockelmann, F. D., Callies, U., Gerdts, G., Wichels, A., Wiltshire, K. H., Glöckner, F. O., Schweder, T., and Amann, R.: Substrate-controlled succession of marine bacterioplankton populations induced by a phytoplankton bloom, Science, 336, 608–611, doi:10.1126/science.1218344, 2012.

ter Braak, C. J. F.: Canonical correspondence analysis: a new eigenvector technique for multivariate direct gradient analysis, Ecology, 67, 1167–1179, doi:10.2307/1938672, 1986.

Thompson, A. W., Foster, R. A., Krupke, A., Carter, B. J., Musat, N., Vaulot, D., Kuypers, M. M. M., and Zehr, J. P.: Unicellular cyanobacterium symbiotic with a single-celled eukaryotic alga, Science, 337, 1546–1550, doi:10.1126/science.1222700, 2012.

Torréton, J.-P., Rochelle-Newall, E., Pringault, O., Jacquet, S., Faure, V., and Briand, E.: Variability of primary and bacterial production in a coral reef lagoon (New Caledonia), Mar. Pollut. Bull., 61, 335–348, doi:10.1016/j.marpolbul.2010.06.019, 2010.

BGD
12, 20179–20222, 2015

Tripp, H. J.: The unique metabolism of SAR11 aquatic bacteria, J. Microbiol., 51, 147–153, doi:10.1007/s12275-013-2671-2, 2013.
Tripp, H. J., Bench, S. R., Turk, K. A., Foster, R. A., Desany, B. A., Niazi, F., Affourtit, J. P., and Zehr, J. P.: Metabolic streamlining in an open-ocean nitrogen-fixing cyanobacterium, Nature, 464, 90–94, doi:10.1038/nature08786, 2010.
Turk-Kubo, K. A., Frank, I. E., Hogan, M. E., Desnues, A., Bonnet, S., and Zehr, J. P.: Diazotroph community succession during the VAHINE mesocosms experiment (New Caledonia Lagoon), Biogeosciences Discuss., 12, 9043–9079, doi:10.5194/bgd-12-9043-2015, 2015.
Van Mooy, B. A. S., Rocap, G., Fredricks, H. F., Evans, C. T., and Devol, A. H.: Sulfolipids dramatically decrease phosphorus demand by picocyanobacteria in oligotrophic marine environments, P. Natl. Acad. Sci. USA, 103, 8607–8612, doi:10.1073/pnas.0600540103, 2006.
Van Mooy, B. A. S., Fredricks, H. F., Pedler, B. E., Dyhrman, S. T., Karl, D. M., Koblízek, M., Lomas, M. W., Mincer, T. J., Moore, L. R., Moutin, T., Rappé, M. S., and Webb, E. A.: Phytoplankton in the ocean use non-phosphorus lipids in response to phosphorus scarcity, Nature, 458, 69–72, doi:10.1038/nature07659, 2009.
Van Wambeke, F., Pfreundt, U., Barani, A., Berthelot, H., Moutin, T., Rodier, M., Hess, W. R., and Bonnet, S.: Heterotrophic bacterial production and metabolic balance during the VAHINE mesocosm experiment in the New Caledonia lagoon, Biogeosciences Discuss., 12, 19861–19900, doi:10.5194/bgd-12-19861-2015, 2015.
Veldhuis, M. J., Kraay, G. W., Van Bleijswijk, J. D., and Baars, M. A.: Seasonal and spatial variability in phytoplankton biomass, productivity and growth in the northwestern Indian Ocean: the southwest and northeast monsoon, 1992–1993, Deep-Sea Res. Pt. I, 44, 425–449, 1997.
West, N. J., Obernosterer, I., Zemb, O., and Lebaron, P.: Major differences of bacterial diversity and activity inside and outside of a natural iron-fertilized phytoplankton bloom in the Southern Ocean, Environ. Microbiol., 10, 738–756, doi:10.1111/j.1462-2920.2007.01497.x, 2008.
Wong, M.-T. and Liu, W.-T.: Ecophysiology of Defluviicoccus-related tetrad-forming organisms in an anaerobic-aerobic activated sludge process, Environ. Microbiol., 9, 1485–1496, doi:10.1111/j.1462-2920.2007.01267.x, 2007.
Wong, M.-T., Tan, F. M., Ng, W. J., and Liu, W.-T.: Identification and occurrence of tetrad-forming Alphaproteobacteria in anaerobic-aerobic activated sludge processes, Microbiology+, 150, 3741–3748, doi:10.1099/mic.0.27291-0, 2004.

BGD
12, 20179–20222, 2015

Yin, Q., Fu, B., Li, B., Shi, X., Inagaki, F., and Zhang, X.-H.: Spatial variations in microbial community composition in surface seawater from the ultra-oligotrophic center to rim of the South Pacific Gyre, PloS One, 8, e55148, doi:10.1371/journal.pone.0055148, 2013.

Zwirglmaier, K., Jardillier, L., Ostrowski, M., Mazard, S., Garczarek, L., Vaulot, D., Not, F., Massana, R., Ulloa, O., and Scanlan, D. J.: Global phylogeography of marine Synechococcus and Prochlorococcus reveals a distinct partitioning of lineages among oceanic biomes, Environ. Microbiol., 10, 147–161, doi:10.1111/j.1462-2920.2007.01440.x, 2008.

BGD
12, 20179–20222, 2015

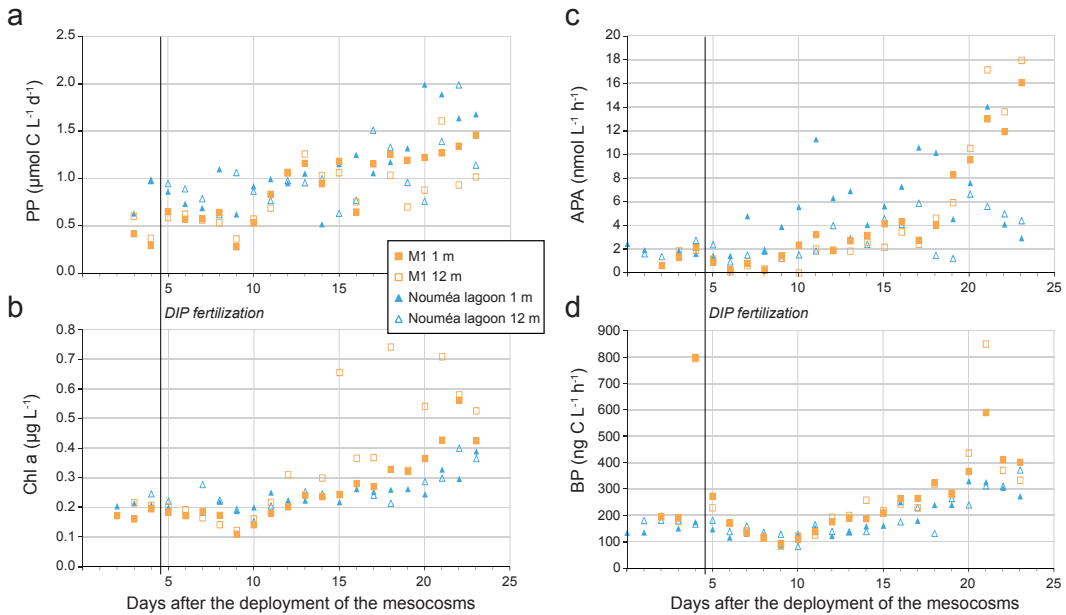

Figure 1. Evolution of selected parameters in mesocosm M1 and the Nouméa lagoon at depths of 1 and 12 m. **(a)** Primary production (PP), **(b)** chlorophyll *a* (chl *a*) concentration, **(c)** alkaline phosphatase activity (APA) and **(d)** heterotrophic bacterial production (BP, measured by ^{3}H-leucine assimilation).

BGD
12, 20179–20222, 2015

Succession within the prokaryotic communities during the VAHINE mesocosms

U. Pfreundt et al.

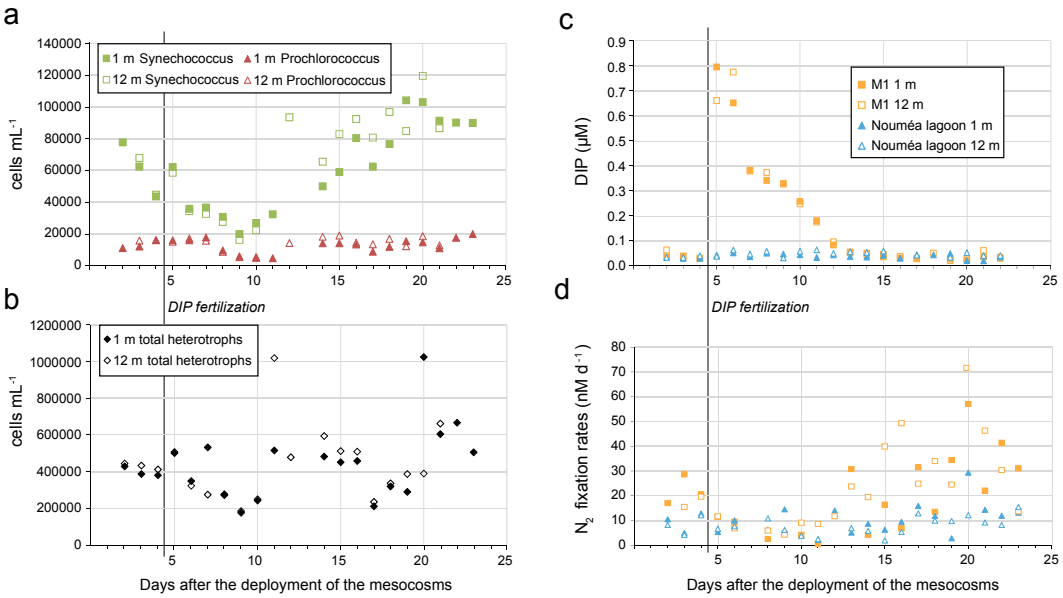

Figure 2. Evolution of absolute abundances in M1 at depths of 1 and 12 m of **(a)** *Synechococcus* and *Prochlorococcus* and **(b)** non-photosynthetic bacteria (total heterotrophs) as measured by flow cytometry. Evolution of **(c)** dissolved inorganic phosphorous (DIP) and **(d)** N_2 fixation rates as measured by ^{15}N incorporation in M1 and the Nouméa lagoon at depths of 1 and 12 m.

BGD
12, 20179–20222, 2015

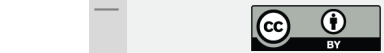

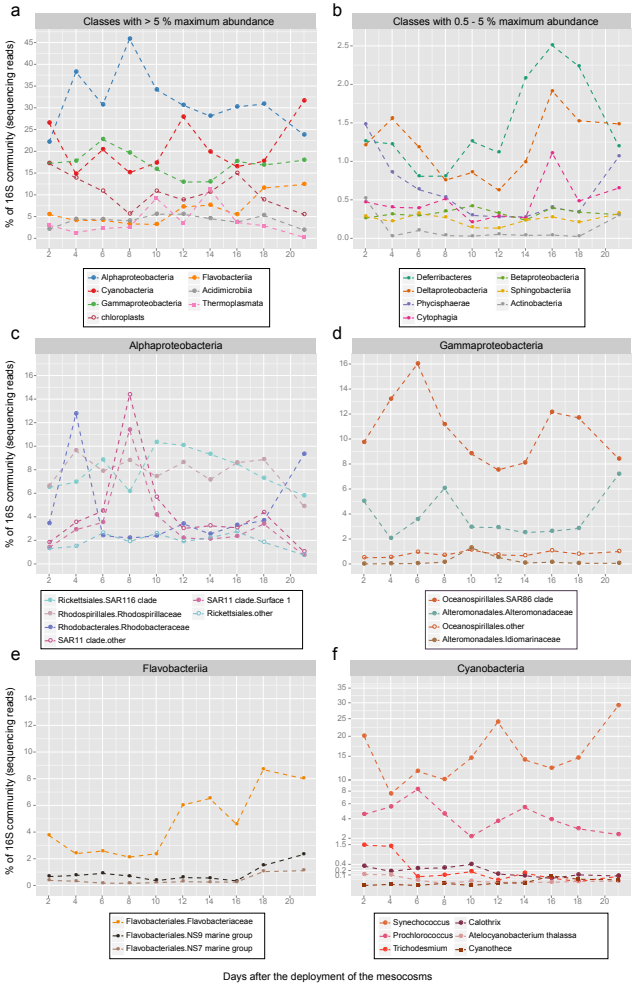

BGD
12, 20179–20222, 2015

Succession within the prokaryotic communities during the VAHINE mesocosms

U. Pfreundt et al.

Figure 3. Evolution of the 16S community with time for surface samples (1 m depth) inside mesocosm M1. All abundances are given as a percentage of total 16S reads. For better visualization, the classes with **(a)** a maximum abundance above 5 % and **(b)** a maximum abundance between 0.5–5 % were plotted separately. **(c–e)** Families with > 1 % of total 16S reads (at their respective maximum) amongst the dominant non-photosynthetic classes *Alphaproteobacteria*, *Gammaproteobacteria*, and *Flavobacteriia*. **(f)** All genera > 0.05 % of total 16S reads (at their respective maximum) within photosynthetic *Cyanobacteria*. Dashed lines were used to connect the data points for better visualization only.

BGD
12, 20179–20222, 2015

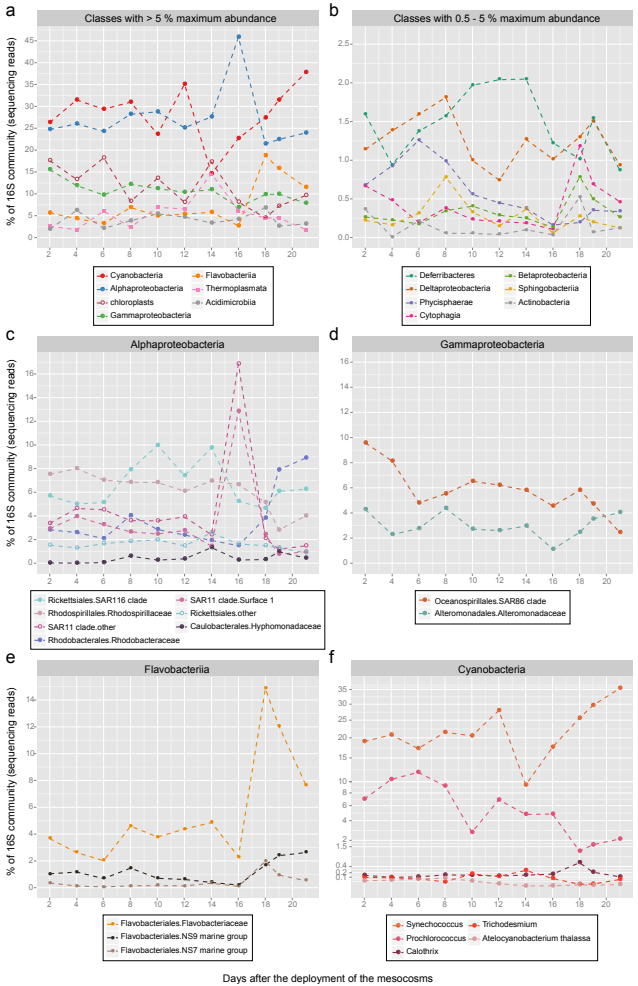

BGD
12, 20179–20222, 2015

Succession within the prokaryotic communities during the VAHINE mesocosms

U. Pfreundt et al.

Figure 4. Evolution of the 16S community with time for surface samples in the Nouméa lagoon waters. All abundances are given as a percentage of total 16S reads. Data was plotted in the same way as for Fig. 2.

BGD
12, 20179–20222, 2015

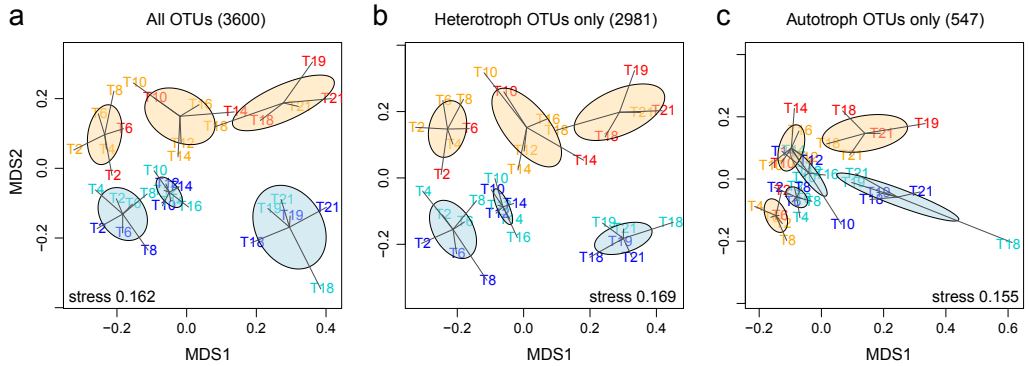

Figure 5. NMDS ordination of all samples using Bray–Curtis distances based on the relative abundances of **(a)** all OTUs, **(b)** only non-cyanobacterial OTUs ("heterotrophic bacteria"), or **(c)** only OTUs classified as photosynthetic cyanobacteria. The samples are color-coded as follows: orange – M1 surface, red – M1 12 m, light blue – Nouméa lagoon surface, blue – Nouméa lagoon 12 m. Ellipses are color coded in a similar way to distinguish M1 sample clusters and Nouméa lagoon sample clusters. Ellipses denote a confidence interval of 0.95 around the weighted average of each cluster. Thus, clusters can be considered significantly different with alpha = 0.05, if ellipses do not overlap.

BGD
12, 20179–20222, 2015

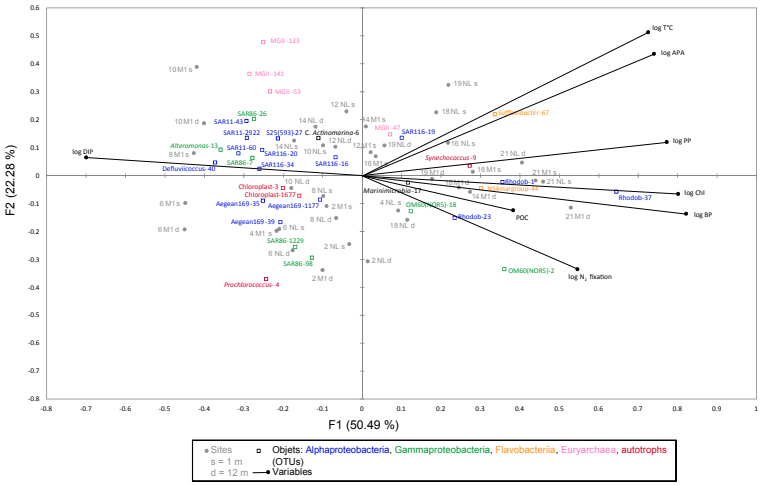

Figure 6. Canonical correspondence analysis of bacterial 16S community structure. Gray full circles are "sites" coded "M1" and "NL" for their origin from mesocosm M1 and the Nouméa lagoon, then "s" or "d", according to the depth sampled (1 and 12 m, respectively). These codes are prefixed by a number according to the day of sampling (from day 2 to day 21). Color coded open squares mark the 34 most abundant OTUs in the two-dimensional space of the plot. These were one *Synechococcus*, one *Prochlorococcus*, and two chloroplast OTUs (autotrophs, red); three SAR11, four SAR116, three Aegean169 marine group, three not further classified *Rhodobacteraceae* (Rhodob), one *Rickettsiales* S25 (593), and one *Rhodospirillaceae* (*Defluviicoccus*) OTU (alphaproteobacteria, blue); four SAR86, two OM60(NOR5) clade (*Alteromonadaceae)*, and one *Alteromonas* OTU (gammaproteobacteria, green); one *Sufflavibacter* and one NS4 marine group OTU (*Flavobacteriia*, orange); four Marine Group II archaea (MGII, euryarchaea, pink); one Candidatus Actinomarina OTU (Acidimicrobiales, black) and one unclassified *Marinimicrobia* OTU (black). Correlations between environmental variables and the first two CCA axes are represented by the lengths and angles of the arrows. The position of OTUs or samples relative to arrows indicates the extent to which the distribution of that OTU or the community composition of that sample is influenced by the environmental parameter represented by that arrow.

BGD
12, 20179–20222, 2015